ELSEVIER

16 September 1994

Chemical Physics Letters 227 (1994) 461–466

CHEMICAL
PHYSICS
LETTERS

Nascent state-resolved ClO in reactions and photodissociation processes

S. Baumgärtel, K.-H. Gericke

Universität Frankfurt/Main, Marie-Curie-Strasse 11, D-60439 Frankfurt/Main, Germany

Received 22 June 1994; in final form 15 July 1994

Abstract

We report a detection technique for the complete state-resolved observation of nascent ClO generated in the photodissociation of parent molecules or formed as product in chemical reactions. The sensitivity and resolution of the applied (2+1) laser-induced fluorescence technique is demonstrated in the photodissociation of ClO_2 at 337–360 nm and in the important atmospheric reaction of Cl with O_3. In the photodissociation of ClO_2, ClO is observed in lower vibrational states ($v=0, 1, 2$). The rotational temperature is found to be 650 ± 60 K ($v=0$). ClO from the reaction of Cl with O_3 is generated mainly in higher vibrational states ($v=3, 4$).

1. Introduction

This Letter demonstrates resonant two-photon laser excitation and one-photon VUV fluorescence detection, (2+1) LIF, of nascent chlorine monoxide radical produced in the photodissociation of ClO_2 and in the reaction of O_3 with Cl. This radical is of great interest because of its central role in the chlorine cycle of stratospheric ozone depletion [1–4].

ClO was first observed in ultraviolet emission spectra from chlorine seeded flames [5]. Later, it was the object of flash photolysis studies [6–8]. Other workers observed absorption spectra between 250 and 310 nm corresponding to the $A\,^2\Pi\leftarrow X\,^2\Pi$ transition of ClO [9,10]. Diode laser detection of the ClO ground state [11], millimeter wavelength measurements [12,13] and a detailed absorption measurement of the $C\,^2\Sigma\leftarrow X\,^2\Pi$ transition [14] have contributed to a firm set of precise vibrational and rotational constants of ClO.

Thus the ClO radical is well known in terms of its spectroscopy. However, absorption measurements are in general not suitable for detecting nascent product molecules because of the low sensitivity. The resonance-enhanced multi-photon ionization method (REMPI) overcomes this problem and this technique was used for the nascent detection of ClO from dissociation processes by exciting the $C\,^2\Sigma$, $D\,^2\Sigma$, $E\,^2\Sigma$ and $F\,^2\Sigma$ electronic states [15,16]. However, the published spectra show a low resolution and are not suitable for obtaining rotational distributions of ClO. In addition, the REMPI technique can hardly be used to obtain spectra of nascent ClO originating as a product of chemical reactions, such as the important reaction of Cl with O_3 as the primary part of the ozone depletion cycle. The sensitive laser induced fluorescence (LIF) technique has not been used for observing ClO, because the first excited state of ClO, $A\,^2\Pi$, is predissociative [17–19]. The second known excited state, $C\,^2\Sigma$, is not predissociative, but requires an excitation wavelength of 170 nm which is not available from tunable dye lasers.

In this Letter, we report a resonant two-photon excitation of $ClO(X\,^2\Pi)$ to the $ClO(C\,^2\Sigma)$ excited state.

SSDI 0009-2614(94)00863-9

The required wavelength around 340 nm is easily available with today's laser systems. The VUV resonant fluorescence from the excited state to the ground state ($C\,^2\Sigma \rightarrow X\,^2\Pi$) around 170 nm is measured without spectral dispersion. This two-photon (2+1) LIF technique allows a sensitive and high resolving observation of nascent ClO.

2. (2+1) LIF spectroscopy of ClO

The following mechanism for observing the ClO fragment in the one-colour photodissociation experiment of ClO_2 takes place:

$$OClO(\tilde{X}\,^2B_2) + h\nu(340\,\text{nm}) \rightarrow OClO(\tilde{A}\,^2A_2)\,, \quad (1)$$

$$OClO(\tilde{A}\,^2A_2) \rightarrow ClO^*(X\,^2\Pi_i) + O(^3P)\,, \quad (2)$$

$$ClO^*(X\,^2\Pi_i) + 2h\nu(340\,\text{nm}) \rightarrow ClO(C\,^2\Sigma)\,, \quad (3)$$

$$ClO(C\,^2\Sigma) \rightarrow ClO(X\,^2\Pi) + h\nu(170\,\text{nm})\,. \quad (4)$$

The first step (Eq. (1)) is the excitation of chlorine dioxide from the $\tilde{X}\,^2B_2(0,0,0)$ ground state to rovibrational levels of the $\tilde{A}\,^2A_2(\nu_1, \nu_2, \nu_3)$ state. This prepared $\tilde{A}\,^2A_2(\nu_1, \nu_2, \nu_3)$ state predissociates due to an interaction with the close-lying $\tilde{A}\,^2A_1$ state [20] leading to $ClO(X\,^2\Pi)$ and $O(^3P)$ (Eq. (2)). The next step (Eq. (3)) is the resonant two-photon excitation of $ClO(X\,^2\Pi)$ to the $ClO(C\,^2\Sigma)$ state. Finally, $ClO(C\,^2\Sigma)$ is deactivated to the electronic ground state under emission of a 170 nm photon.

In a two-photon process $\Delta J = \pm 2$ transitions are also allowed and the resulting O and S branches cause a more complicated spectrum in comparison to one-photon LIF. In addition, the spin–orbit coupling leads to the two systems $^2\Pi_{3/2}$ and $^2\Pi_{1/2}$. Thus, five main branches (O, P, Q, R, S) are expected for each spin-orbit system. Furthermore, ClO(C–X) is an intermediate between Hund's case a and b. Only in the high J limit ClO is characterized as Hund's case b. As a consequence, the five satellite lines, $^PO_{21}$, $^QP_{21}$, $^RQ_{21}$, $^SR_{21}$ and $^TS_{21}$ (which violate the $\Delta N = \Delta J$ selection) are expected for the $^2\Pi_{3/2}$ system and for the $^2\Pi_{1/2}$ system the $^NO_{12}$, $^OP_{12}$, $^PQ_{12}$, $^QR_{12}$ and $^RS_{12}$ satellite lines must be considered. However, it should be mentioned that the intensities of these lines will be small. In total, there are 20 rotational branches of ClO which must be considered in the two-photon excitation of ClO. The level scheme and all transitions for the two-photon excitation of ClO(C←X) are shown in Fig. 1 where the parity selection rule +↔+ −↔− is considered. The Hönl-London factors for a two-photon transition have been calculated [21] using the spectroscopic constants of Refs. [11,14,22].

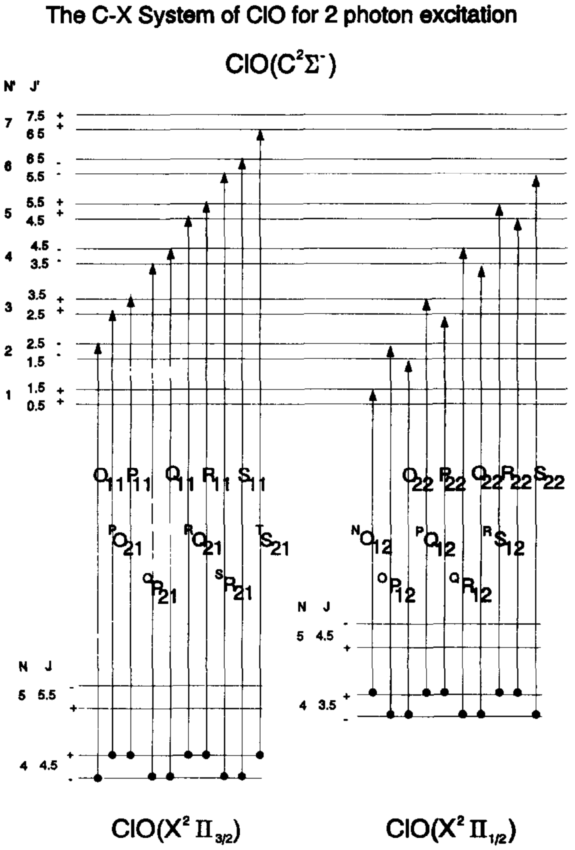

Fig. 1. Level scheme and transitions of the $C\,^2\Sigma^-$–$X\,^2\Pi$ system of ClO for two-photon excitation. The energy splitting of the levels is completely unscaled.

The Franck-Condon factors describe the overlap between the vibronic wavefunction of the X and C states and, therefore, are assumed to be the same as for a one-photon process. The values are given in Ref. [8]. A spectrum simulation of a (2+1) LIF scan of $^{35}ClO(C\,^2\Sigma\ v'=0,\ J') \leftarrow {}^{35}ClO(X\,^2\Pi\ v=0,\ J)$ is shown in the lower part of Fig. 3 where a Gaussian lineshape function ($\Delta\lambda = 0.002$ nm) and a rotational temperature of $T = 650$ K is used.

3. Experimental

The laser pulse for exciting ClO to its $C\,^2\Sigma$ state was delivered by a dye laser (Lambda FL 3000E) pumped by a XeCl excimer laser (Lambda LPX 100). With PTP, dissolved in dioxane, as the active medium of the dye laser, a tuning range of 337–346 nm was achieved and with DMQ, dissolved in dioxane, a tuning range of 345–360 nm was achieved. The typical output power was 10–13 mJ, depending on the dye used at a laser bandwidth of 0.4 cm^{-1}. In addition, high resolution measurements of the lines were made by using a stepping motor tuned intracavity etalon, which limited the bandwidth of the laser radiation to 0.06 cm^{-1}. The laser output energy was monitored during the scans for normalizing the spectra to the laser intensity.

The laser beam was focused by a 50 cm quartz lens into the reaction chamber. Fluorescence was observed with a CsI solar blind photomultiplier (EMR-542G-08-18) perpendicular to the laser beam. The fluorescence radiation around 170 nm is not absorbed to an amount worth mentioning by the molecules in the reaction chamber. The photomultiplier output was fed into a boxcar averager (Standford Research Systems 250) and stored in a microcomputer (AT-386) after A/D conversion. A four channel trigger device (Standford Research Systems DG 535) controlled all time events in the experiment.

ClO_2 was produced by pumping a mixture of chlorine (Matheson) and nitrogen (Linde) (1:10) through a column packed with sodium chlorite (Merck) [23]. The gas mixture was pumped without further purification directly through the reaction chamber. From absorption measurements, we calculate the yield of ClO_2 to be at least 70% of the theoretical value. Chlorine and nitrogen, also present in the gas mixture, do not affect the (2+1) LIF process at the wavelengths used. The total cell pressure was 60 Pa, the partial pressure of ClO_2 was calculated to be at least 4.2 Pa. Under these experimental conditions and a maximum lifetime of the excited ClO below 30 ns we can exclude collisions between photolysis and detection.

We have also monitored the ClO generated in the fast ($k = 2\times10^{-11}$ $cm^3\,s^{-1}$) [24,25] reaction of Cl with O_3. In that case Cl was produced in the photolysis of Cl_2 near the maximum of the first UV-absorption spectrum. The radiation at 351 nm was delivered by a XeF excimer laser (Lambda 201MSC). Ozone was synthesized in a silent discharge from oxygen (Linde) [26]. The ratio of Cl_2:O_3 was 30 Pa:60 Pa.

4. Results and discussion

The observed ClO LIF spectrum resulting from the one-colour experiment in the dissociation of ClO_2 is

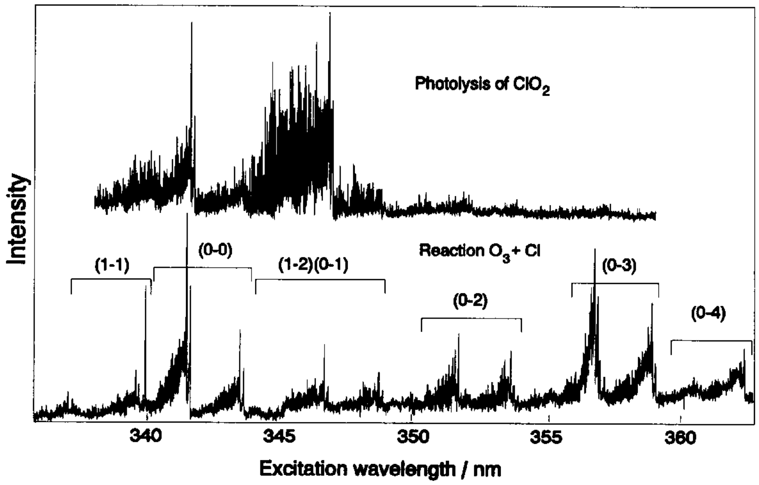

Fig. 2. Upper part: nascent LIF spectrum of ClO from the photodissociation of ClO_2 at 338–360 nm. Lower part: LIF spectrum of ClO from the reaction of Cl with O_3. Cl was prepared in the Cl_2 photodissociation at 351 nm. The ClO reaction product was observed 2.5 µs after photolyzing Cl_2. The assignments of the (v'–v) vibrational transitions are given in brackets.

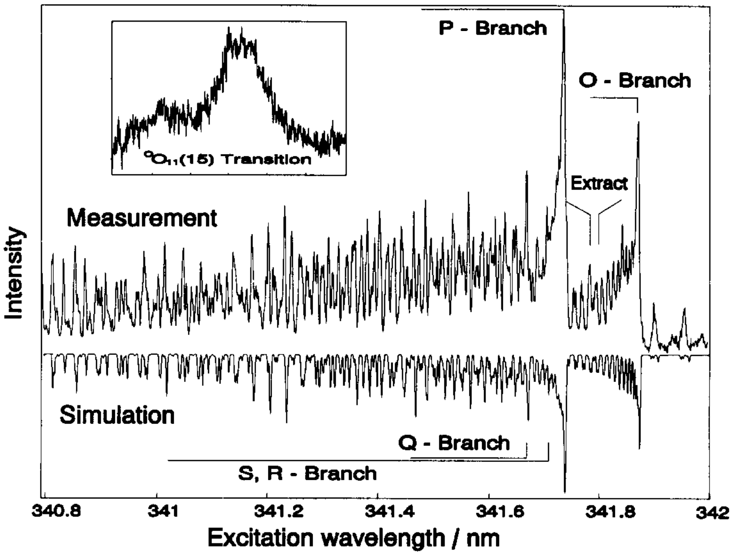

Fig. 3. Upper part: nascent LIF spectrum of the ClO($C\,^2\Sigma$, $v'=0$)←ClO($X\,^2\Pi_{3/2}$, $v=0$) transition at a resolution of 0.6 cm^{-1}. A high resolution scan of the $^{O}O_{11}(15)$ line of the vibrational 0–0 transition is shown in the upper left corner. The bandwidth of the laser was reduced to 0.06 cm^{-1}. Lower part: calculated spectrum of the ^{35}ClO($C\,^2\Sigma$, $v'=0$)←^{35}ClO($X\,^2\Pi_{3/2}$, $v=0$) transition. A Boltzmann distribution of 650 K for the rotational states is used.

represented in the upper scan in Fig. 2. The assignments of the (v'–v) vibrational transitions can easily be performed by comparing the simulated and the measured spectra. The strongest spectral features are the $v'=0$–$v=0$ and $v'=0$–$v=1$ transitions. The upper part of Fig. 3 shows an extract of the spectrum in the upper part of Fig. 2 in the region where the rotational lines of the ClO($C\,^2\Sigma$, $v'=0$)←ClO($X\,^2\Pi_{3/2}$, $v=0$) transition occur. The picture in the upper left edge of that figure shows a single transition $^{O}O_{11}(15)$ recorded with the etalon equipped laser. The observed linewidth (fwhm) is $\Delta\nu_{exp}=0.2$ cm^{-1}. The expected linewidth can be calculated from the available energy, the rotational energy of that probed state and the center frequency of transition. Since the resolution of the dye laser will slightly increase the calculated Doppler width of $\Delta\nu_{cal}=0.18$ cm^{-1}, the experimental value $\Delta\nu_{exp}$ is in excellent agreement with $\Delta\nu_{cal}$.

By comparing our simulation (lower part of Fig. 3) with the spectrum shown in the upper part of Fig. 3, we assigned the structure at the low-energy edge to the band head of the O branch, the second structure to the P band head followed by the R, Q and S band structures. Because of the high line density (rotational constant $B=0.62$ cm^{-1}) and the additional O and S branches of the LIF spectrum, we determined the rotational distribution by fitting the simulated spectrum to the measured spectrum by a least-squares fit procedure. The theoretical line intensity is assumed to be

$$I_{theo}(\nu)=\sum AP(q)S_{q'q}L(\nu_{q'q}-\nu_0,\Delta\nu)\,,$$

where $P(q)$ is the (required) population of the quantum state q, $S_{q'q}$ is the transition probability for $q'\leftarrow q$ transition and $L(\nu_{q'q}-\nu_0,\Delta\nu)$ is the Gaussian lineshape function centered at $\nu=\nu_{q'q}$ with a width of $\Delta\nu$. The summation involves all transitions $q'\leftarrow q$ which contribute to the signal at frequency ν. With that procedure, we obtain the population of each quantum state. A representation of $P(J)$ in a Boltzmann plot (Fig. 4) shows that a rotational temperature parameter of approximately 650 ± 60 K describes the rotational product state distribution in the lowest vibrational state.

As can be seen from Fig. 2, ClO is observed in the one-colour photodissociation of ClO_2 in the $v=0$–2 vibrational states. It should be mentioned that several vibrational levels of the $\tilde{A}\,^2A_2$ state of ClO_2 are excited when the dye laser is scanned over the rovibrational transitions of ClO($C\,^2\Sigma^-\leftarrow X\,^2\Pi$). In a (one-colour) REMPI study of the photodissociation

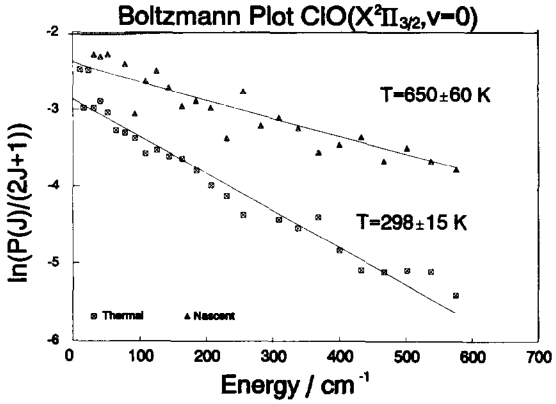

Fig. 4. Boltzmann plot of the rotational distribution of ClO. The upper curve represents ClO product in the photodissociation of ClO_2 where the spectrum shown in Fig. 3 is used. The lower curve represents the rotational distribution of relaxed ClO (Fig. 5).

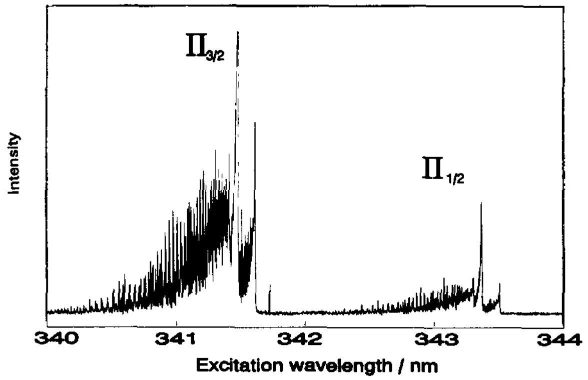

Fig. 5. LIF spectrum of the $ClO(C\,^2\Sigma, v'=0) \leftarrow ClO(X\,^2\Pi, v=0)$ transition, recorded 200 μs after Cl_2 photolysis at a pressure of 2 kPa (argon). Under these conditions only transitions belonging to $v=0$ are observed.

of ClO_2 Vaida and co-workers [15] observed ClO in $v=0$–6 vibrational states. Their spectra in the region between 345 and 360 nm (transitions originating from $v>3$) are 10 times less intense than in the region between 335 and 345 nm (transitions originating from $v<4$). The reduced intensity was attributed to a change from a (2+1) to a (2+2) REMPI process. We should even better observe these transitions, because their reasoning should prefer the LIF process. However, we did not observe any transitions belonging to $v=3$ or higher vibrational states. That the present technique is suitable to detect high vibrational $ClO(X\,^2\Pi)$ states will be demonstrated below where the reaction $Cl+O_3$ is studied.

A part of the LIF spectrum of ClO followed by the reaction of Cl with O_3 is shown in the lower part of Fig. 2. The delay time between photolysis and detection laser beam was 2.5 μs. Under these experimental conditions (≈15 gas kinetic collisions) the rotational distribution is relaxed, but the vibrational distribution should not be strongly affected. ClO is found in $v=0$–5 vibrational states, with a maximum at $v=3$ and $v=4$ (the Franck–Condon factors are ≈3 respectively 6 times smaller than for the other transitions). In an old flash lamp photolysis ClO was observed exclusively in the $v=0$ state [27] but those experimental conditions were insufficient for observing vibrationally unrelaxed products. A trajectory study of the $Cl+O_3$ reaction predicted a significantly vibrationally excited ClO peaking at $v=1$ [28]. We observe an even higher vibrationally excited ClO. In any case, the observation of ClO in vibrational states up to $v=5$ indicates the possibility of ClO detection in highly excited rovibrational states.

By adding an excess of argon (200 Pa) to the reaction chamber and increasing the delay time between photolysis and detection laser beam up to 250 μs, we have observed completely relaxed ClO and the obtained spectrum is shown in Fig. 5. The only populated vibrational level is $v=0$. The two spin–orbit systems are populated at a ratio of 0.25:1 ($\Pi_{1/2}$:$\Pi_{3/2}$) which is in good agreement with the calculated ratio of 0.22:1 ($\Pi_{1/2}$:$\Pi_{3/2}$) for a Boltzmann distribution at $T=300$ K. The rotational temperature was found to be 298±15 K from a fit of the rotational distribution of the $\Pi_{3/2}$ spin system (Fig. 4), which demonstrates the quality of the measurements and the fit procedure.

5. Summary

We have demonstrated that chlorine monoxide can be easily observed by a two-photon LIF process. With this technique completely state-resolved spectra of nascent ClO resulting from photodissociation as well as from reactions can be observed. The resolution and sensitivity of the present ClO detection is much better than that of spectra obtained with other known techniques. Actually, we set up experiments to investigate the dissociation of ClO_2 and Cl_2O at fixed dissociation wavelengths in order to study the dynamics of fragmentation from single selected vibrational (ν_1, ν_2, ν_3) levels. The detailed investigations of ClO produced in the reaction of Cl with O_3 as well as in the reaction of $O(^1D)$, $O(^3P)$ with HCl will be published in a forthcoming paper.

Acknowledgement

Support of the Deutsche Forschungsgemeinschaft is gratefully acknowledged. We thank Professor Dr. F.J. Comes for material support and helpful discussions.

References

[1] R.S. Stolarski and R.J. Cicerone, Can. J. Chem. 52 (1974) 1610.
[2] M.J. Molina and L.T. Molina, J. Phys. Chem. 91 (1987) 433.
[3] M.J. Prather and R.T. Watson, Nature 344 (1990) 729.
[4] J.G. Anderson, D.W. Toohey and W.H. Brune, Science 251 (1991) 29.
[5] G. Pannetier and A.G. Gaydon, Nature 161 (1948) 242.
[6] J.B. Nee and K.J. Hsu, J. Photobiol. A 55 (1991) 269.
[7] C.M. Humphries, A.D. Walsh and P.A. Warsop, Discussions Faraday Soc. 35 (1963) 137.
[8] N. Basco and R.D. Morse, J. Mol. Spectry. 45 (1973) 35.
[9] R.A. Durie and D.A. Ramsay, Can. J. Phys. 36 (1958) 35.
[10] P.W. McLaughin, C.R. Park and J.R. Wiesenfeld, J. Mol. Spectry. 162 (1993) 307.
[11] J.B. Burkholder, P.D. Hammer, C.J. Howard, A.G. Maki, G. Thompson and C. Chackerian, J. Mol. Spectry. 139 (1987) 124.
[12] J.W. Waters, J.C. Hardy, R.F. Jarnot and H.M. Pickett, Science 214 (1981) 61.
[13] M. Solomon, R.L. DeZafra, A. Perrish and J.W. Barrett, Science 224 (1984) 1210.
[14] J.A. Coxon, Can. J. Phys. 57 (1979) 1034.
[15] E. Rühl, A. Jefferson and V. Vaida, J. Phys. Chem. 94 (1990) 2990.
[16] M.T. Duigan and J.W. Hudgens, J. Chem. Phys. 10 (1985) 4426.
[17] M.A.A. Clyne, I.S. McDermid and A.H. Curran, J. Photochem. 5 (1976) 201.
[18] P.R. Bunker and P.C. Klein, Chem. Phys. Letters 78 (1981) 552.
[19] S.A. Barton, J.A. Coxon and U.K. Roychowdhury, Can. J. Phys. 62 (1984) 473.
[20] K.A. Peterson and H.-J. Werner, J. Chem. Phys. 94 (1992) 8948.
[21] J.B. Halpern, H. Zacharias and R. Wallenstein, J. Mol. Spectry. 79 (1980) 1.
[22] G. Herzberg, Spectra of diatomic molecules (VNR, New York, 1950).
[23] W.S. Hutchinson and R.I. Derby, Ind. Eng. Chem. 37 (1945) 813.
[24] M.J. Kurylo and W. Braun, Chem. Phys. Letters 37 (1976) 232.
[25] M.S. Zahniser, F. Kaufman and J.G. Anderson, Chem. Phys. Letters 37 (1976) 226.
[26] K.-H. Gericke, F.J. Comes and R.D. Levine, J. Chem. Phys. 74 (1981) 6106.
[27] W.D. McGrath and R.G.W. Norrish, Z. Physik. Chem. 15 (1958) 245.
[28] S.C. Farantos and J.N. Murrell, Intern. J. Quantum Chem. 14 (1978) 659.